Greedy Principal Flows

National University of Singapore

Sebastian Lie

05 March 2021

Acknowledgements

My 7 soft toys. And my desk lamp for being the light of my life.

Abstract

Principal Flows are a great tool to use when we want to extend the notion of Principal Component analysis to multivariate datasets that we know lie on non-linear manifolds. We restrict this problem to constructing principal flows on hyperspheres. We use a different, easier method to obtain the principal flow that is even closer to its canonical PCA interpretation.

Contents

1 Introduction **5**

1.1 Motivation . . . 5

1.2 Notation . . . 6

1.3 Definitions . . . 7

1.3.1 Vector Fields . . . 7

1.3.2 Logarithm Maps . . . 8

1.3.3 Tangent Space . . . 8

1.3.4 Geodesics . . . 9

1.3.5 Eigenvalues and Eigenvectors . . . 9

1.3.6 Diagonalisation . . . 9

2 Literature Review **11**

2.1 Linear Dimension Reduction . . . 11

2.1.1 Principal Component Analysis . . . 11

2.1.2 Classical MDS, Euclidean Distance . . . 12

2.2 Non-Linear Dimension Reduction . . . 13

2.2.1 Isomap . . . 14

2.2.2 Locally Linear Embeddding . . . 15

2.2.3 Principal Geodesic Analysis . . . 16

3 Greedy Principal Flows **18**

3.1 Goal Of Research 18

3.2 An explanation of the algorithm 19

3.3 Algorithm Steps 20

3.4 Extension: Greedy Principal Boundary 21

4 Applications **24**

4.1 Toy Data 24

4.1.1 Without Noise 24

4.1.2 With Noise 26

4.1.3 Boundary Flow with Noise 27

4.2 Real World Data 27

4.2.1 MNIST 28

4.2.2 Fashion MNIST 29

4.2.3 Olivetti faces 30

4.2.4 Faces in the Wild 31

4.3 Corrections 32

4.3.1 Abstract 32

4.3.2 Motivation 33

4.3.3 Definitions 33

Chapter 1

Introduction

1.1 Motivation

With the advent of Big Data, and the rise of data science, machine learning has been used successfully to solve a variety of problems, such as regression and classification problems. However, machine learning can also be used in a more subtle, but no less important way: to discover patterns in the data and glean more information from it. Among methods that have this aim, Principal Component Analysis is the most popular, taught in almost every machine learning course. It does however, have a glaring weakness: it does not perform well when the data we are working with is sampled from a non-linear manifold. This, however is fixed with the principal flow algorithm: it constructs a curve that at each local point moves in the direction of maximal variation and retains canonical PCA interpretation in euclidean space. Yet, this method is not easy to obtain, having to solve a problem in variational calculus. What if we could construct this curve with a greedy approach?

1.2 Notation

Notation	**Explanation**
$\mathbb{R}^D$	D dimensional euclidean space.
$\mathbf{X}$	Data matrix of dimensions $n \times D$
D	Dimension of the high-dimensional data.
d	Dimension of the manifold embedded in D dimensional space
$\mathcal{M}^d$	Denotes a connected and complete d-dimensional manifold embedded in $\mathbb{R}^D$
p	A point on the manifold, $\mathcal{M}^d$.
$\mathbf{v}$	A vector.
$T_p\mathcal{M}$	The Tangent space of a point p on $\mathcal{M}^d$.
$\mathbf{C}$	A Covariance matrix.
$\{x_1, ...x_n\}$	A collection of n data points in D dimensions.
$\mathbf{1}$	A vector of 1s.
$\mathbf{I}$	The identity matrix.
$\mathbf{X}^T$	Transpose of a some matrix $\mathbf{X}$.
$\mathbf{X}_{(d)}$	Transpose of a some matrix $\mathbf{X}$.
$\mathbf{M}$	Dissimilarity Matrix, dimension $n \times n$

1.3 Definitions

1.3.1 Vector Fields

A vector at point $\mathbf{x}$, $\mathbf{x} \in \mathbb{R}^D$ is a pair $\mathbf{a} = (\mathbf{x}, \mathbf{v})$, $\mathbf{v} \in \mathbb{R}^D$, such that $\mathbf{v}$ is the vector $\mathbf{v}$ translated so that its tail is at $\mathbf{x}$ instead of the origin. All vector operations are defined such that the first item of the pair remains the same, and the second item is the result of the operation. The length and angle between two vectors are the same as normal vectors rooted in the origin.

Definition: A *vector field* $\mathbf{F}$ on $U \subset \mathbb{R}^D$ is a function which assigns to each point of U a vector at that point. Then

$$\mathbf{F}(\mathbf{x}) = (\mathbf{x}, F(\mathbf{x}))$$

for some function $F : U \longrightarrow \mathbb{R}^D$. Vector fields on $\mathbb{R}^D$ are often most easily described by specifying this associated function F. A pictoral example of a vector field is below.

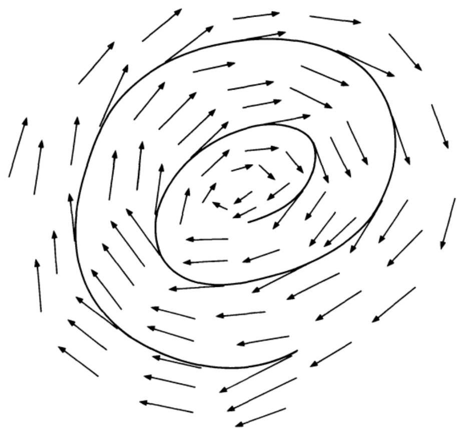

Figure 1.1: An example of a vector field, $\mathbb{R}^3$

1.3.2 Logarithm Maps

Logarithm Map: For each $p \in \mathcal{M}^d$, let

$$log_p(x) : \mathcal{M}^d \longrightarrow T_p\mathcal{M}$$

be the logarithm map. The log map is a function that projects a point x on the manifold $\mathcal{M}^d$ onto $T_p\mathcal{M}$, by producing a vector on $T_p\mathcal{M}$ which indicates the direction in which p should move to obtain the projection of $x \in \mathcal{M}^d$ onto $T_p\mathcal{M}$.

Exponential Map: For each $p \in \mathcal{M}^d$, let

$$exp_p(\mathbf{v}) : T_p\mathcal{M} \longrightarrow \mathcal{M}^d$$

be the exponential map. Exponential maps are the inverse of the logarithm maps. Let the vector $\mathbf{v}$ be the vector from p to the point t on $T_p\mathcal{M}$ we wish to project onto $\mathcal{M}^d$. Then the exponential map moves along the geodesic on $\mathcal{M}^d$ that mirrors the direction of $\mathbf{v}$ on $T_p\mathcal{M}$ and finds the projection of t on $\mathcal{M}^d$.

1.3.3 Tangent Space

To define the tangent space we refer to the diagrams below.

Let the sphere be the manifold, $\mathcal{M}^d$, and let $T_p\mathcal{M}$ be the plane tangent to $\mathcal{M}^d$. Let the blue point be p. This is to say that the tangent space of some manifold $\mathcal{M}^d$ log_p would then project points from $\mathcal{M}^d$ to the hyperplane, and exp_p would project points from $T_p\mathcal{M}$, the hyperplane, to $\mathcal{M}^d$. Any vectors lying in this hyperplane are in the tangent space, of $\mathcal{M}^d$ at p.

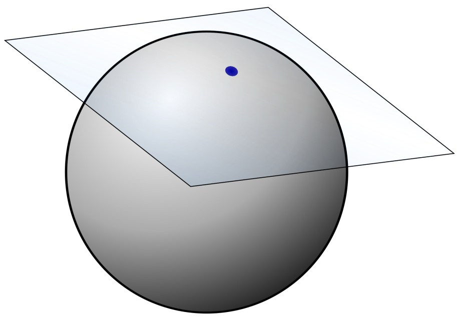
(a) Tangent Space of a Sphere

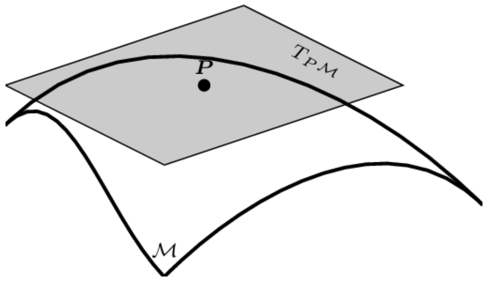

(b) Close-up of the Tangent space in (a)

Figure 1.2: Illustration of a Tangent Space

1.3.4 Geodesics

Geodesics are curves on $\mathcal{M}^d$ which play the same role as straight lines in $\mathbb{R}^d$. They can be thought of as the "shortest path" between 2 points on the manifold, $\mathcal{M}^d$.

The Euclidean distance between 2 points p, q is defined as $\|p - q\|$, or the 2-norm of the vector $p - q$. Geodesic distance extends this concept of Euclidean, straight line distance in the Euclidean space to Manifolds.

1.3.5 Eigenvalues and Eigenvectors

Now we define eigenvalues and eigenvectors.

Definition: Let $\mathbf{A} \in \mathbb{R}^{n \times n}$. Then a non-zero vector $\mathbf{v}$ is an eigenvector of $\mathbf{A}$ if there exists some scalar λ such that $\mathbf{Av} = \lambda\mathbf{v}$. Then λ is known as the eigenvalue corresponding to vector $\mathbf{v}$.

Here we also note that for any 2 eigenvectors v_i and v_j, $i \neq j$, $v_i \cdot v_j = 0$, or any 2 eigenvectors are orthogonal to each other, and that $v_i \cdot v_i = 1$.

1.3.6 Diagonalisation

We say that a matrix is diagonalisable if $\exists\mathbf{V}$, an orthonormal matrix such that the rows of $\mathbf{V}$ are the eigenvectors of $\mathbf{C}$, and a diagonal matrix $\mathbf{E}$ whose diagonal entries are the eigenvalues of $\mathbf{C}$. In the context of this report, we only consider the eigendiagonalisation of some covariance matrix $\mathbf{C} \in \mathbb{R}^{D \times D}$, which is symmetric and thus, always diagonalisable. Formally, the eigendiagonalisation of $\mathbf{C}$ is given by:

$$\mathbf{C} = \mathbf{V}\mathbf{E}\mathbf{V}^T$$

Chapter 2

Literature Review

2.1 Linear Dimension Reduction

2.1.1 Principal Component Analysis

Principal Component analysis tries to obtain a lower-dimensional representation of the data that retains as much variation as possible present in the data set. PCA relies on constructing principal components (PCs): new variables that are linear combinations of the original variables that have first been centered. These PCs are uncorrelated (orthogonal) and ordered in descending order by the amount of variability of the original data retained. It reduces some high-dimensional data of dimension D to d by computing the first d PCs in the process below:

```
Result: Write here the result
initialization;
while While condition do
    instructions;
    if condition then
        instructions1;
        instructions2;
    else
        instructions3;
    end
end
```

Algorithm 1: How to write algorithms

Algorithm

1. First we center the data matrix, $\mathbf{X}$.
2. Next we compute the covariance matrix of the centered data matrix: $\mathbf{C}$.
3. Now we compute the eigendiagonalisation of $\mathbf{C}$, and obtain $\mathbf{V}_d$, the d eigenvectors associated the d largest eigenvalues.
4. Then constructing the d principal components is done by computing $\mathbf{X}\mathbf{V}_d$.

2.1.2 Classical MDS, Euclidean Distance

Multidimensional Scaling's main aim is to take some D dimensional data, $\mathbf{X} \in \mathbb{R}^{n \times D}$ and find some d dimensional points that minimises the discrepancy in the pairwise distances of the points in the original D dimensional representation and the new d dimensional representation. Let a squared dissimilarity matrix calculated using euclidean distance between n points be given by $\mathbf{M} \in \mathbb{R}^{n \times n}$, (define M in notation) let the matrix of coordinates be denoted by $\mathbf{X} \in \mathbb{R}^{n \times D}$, and let $\mathbf{B} = \mathbf{X}\mathbf{X}^T$ be the gram matrix. Since dissimilarities do not change under translations, we assume that $\mathbf{X}$ has column means equal to 0. MDS seeks to find a lower dimensional representation (define $X_{(d)}$) $\mathbf{X}_{(d)} \in \mathbb{R}^{n \times d}$.

Algorithm:

1. Compute or obtain the dissimilarity matrix, $\mathbf{S}$.

2. Let $\mathbf{J}$ be the centering matrix: $\mathbf{J} = \mathbf{I} - n^{-1}\mathbf{1}\mathbf{1}^T$. Compute $\mathbf{B} = -\frac{1}{2}\mathbf{JSJ}$.

3. Then, compute the eigensdecomposition of $\mathbf{B}$: $\mathbf{B} = \mathbf{V}\boldsymbol{\Lambda}\mathbf{V}^T$.

4. Then $\mathbf{X} = \mathbf{V}\boldsymbol{\Lambda}^{1/2}$ and for a d-dimensional representation of $\mathbf{X}$: $\mathbf{X}_{(d)}$, $\mathbf{X}_{(d)} = \mathbf{V}_d\boldsymbol{\Lambda}_d^{1/2}$, where $\boldsymbol{\Lambda}_d^{1/2}$ is the first $d \times d$ submatrix of Λ, and $\mathbf{V}_d$ is the first d columns of $\mathbf{V}$, i.e the first d eigenvectors and their corresponding eigenvalues.

Note that using Euclidean distances, the result of MDS is the same as PCA.

2.2 Non-Linear Dimension Reduction

Non-linear dimensionality reduction methods are particularly useful when the multivariate data we obtain is sampled from a smooth non-linear manifold $\mathcal{M}^d$, e.g a manifold in an S-shape or a hypersphere. This class of methods obtain better estimates than linear methods like PCA and MDS, especially for the data mentioned above. They are especially successful as certain data sets contain essential nonlinear structures that are invisible to PCA and MDS.

2.2.1 Isomap

Isomap, introduced by Tenenbaum et al. [3] is an extension of MDS to manifolds in which embeddings are optimized to preserve geodesic distances between pairs of data points. It combines the major algorithmic features of PCA and MDS — computational efficiency, global optimality, and asymptotic convergence guarantees — with the flexibility to learn a broad class of nonlinear manifolds. Isomap achieves this by estimating the geodesic distance between data points, given only input-space distances, e.g euclidean distance between points.

This relies on the fact that for neighboring points, input-space distance provides a good approximation to geodesic distance. For faraway points, Isomap approximates geodesic distance by adding up a sequence of "short hops" between neighboring points, computed efficiently by finding shortest paths in a graph with edges connecting neighboring data points. This approximation relies on the proof that for a sufficiently high density of data points, we can always choose a neighborhood size (e or K) large enough that the graph will (with high probability) have a path not much longer than the true geodesic, but small enough to prevent edges that "short circuit" the true geometry of the manifold [3].

Isomap Algorithm:

1. Construct neighbourhood graph G: First, we need to compute the distances between points: for any node i and j, connect the 2 nodes if $d(i, j) < \epsilon$ or if j is one of the k-nearest neighbours of i.

2. Compute all-pairs shortest paths on G. There are many algorithms to do this, but we use the Floyd-Warshall algorithm.

3. Construct a d-dimensional embedding using MDS.

2.2.2 Locally Linear Embeddding

Locally Linear Embedding (LLE) introduced by Saul and Roweis [6] aims to construct a mapping from the D dimensional original points to the d dimensional reconstructed points that preserves the local configurations of each point's nearest neighbors. Locally, LLE assumes the embedding is linear, and for each data point $p \in \mathbb{R}^D$, LLE uses a linear combination of its K nearest neighbours to reconstruct a lower-dimensional $p_d \in \mathbb{R}^d$. LLE does this by first learning some reconstruction weights from the D-dimensional data: $\mathbf{W}$ where $\mathbf{W}_{ij}$ represents the contribution of the j-th data point in reconstructing the i-th one. These weights obey an important symmetry: for any particular data point, they are invariant to rotations, rescalings, and translations of that data point and its neighbors. They thus reflect intrinsic geometric properties of the data that are invariant to such transformations, and therefore, we expect their characterization of local geometry in the original data space to be equally valid for local patches on the manifold. This is what motivates our use of $\mathbf{W}_{ij}$ in reconstructing the embedded manifold coordinates in d dimensions. At the end of LLE, each D-dimensional observation $\mathbf{X}_i$ is mapped to a low dimensional vector $\mathbf{Y}_i$ representing global internal coordinates on the manifold.

LLE Algorithm:

1. Compute the K nearest Neighbors of each original data point $\mathbf{X}_i$ using euclidean distance, where K is a hyperparameter.

2. Compute the weights $\mathbf{W}_{ij}$ that best reconstruct each data point from it's neighbours minimizing the **Reconstruction Error** below by constrained linear fits.

$$\varepsilon(\mathbf{W}) = \sum_i |\mathbf{X}_i - \sum_j \mathbf{W}_{ij}\mathbf{X}_j|^2$$

3. Compute the vectors $\mathbf{Y}_i$ best reconstructed by the weights $\mathbf{W}_{ij}$ by choosing the d

dimensional coordinates of each output that minimise the embedding cost function:

$$\Phi(\mathbf{Y}) = \sum_i |\mathbf{Y}_i - \sum_j \mathbf{W}_{ij}\mathbf{Y}_j|^2$$

Note that $\mathbf{W}_{ij}$ here is fixed, obtained from the previous step.

2.2.3 Principal Geodesic Analysis

Principal Geodesic Analysis(PGA) introduced here [2], is a generalization of principal component analysis to manifolds. The main aim of PGA is to describe some data on $\mathcal{M}^d$ by obtaining some principal geodesics that are analogous to principal directions in PCA: the directions along which data is projected to obtain a principal component. First we qualify what an intrinsic mean is. Let $T_p\mathcal{M}$ be the tangent space of $\mathcal{M}$ at the intrinsic mean p of the x_i. The intrinsic mean of some data $\mathbf{X}$ lying on some manifold is obtained by first setting the initial mean to a random data point, then iteratively obtaining a better estimation of the intrinsic mean by computing the average of the vectors obtained using the log map at the current mean on all data points, then taking the next estimate of the intrinsic mean as the projection of that average using the exponential map at the current estimate.
Instead of finding the principal geodesic however, Fletcher et al. prove that we can approximate the d geodesics along which maximal variation lies by projecting data from $\mathcal{M}^d$ to $T_p\mathcal{M}$ and then finding the d eigenvectors associated with the d largest eigenvalues of the covariance matrix of the projected data.

Algorithm:

1. Obtain the intrinsic mean, $p \in \mathcal{M}^d$ of $\{x_1, ..x_n\}$.

2. Calculate the vectors $u_i = log_p(x_i)$.

3. Calculate the covariance matrix $\mathbf{S} = \frac{1}{n}\sum_{i=1}^{n} u_i u_i^T$.

4. Diagonalise the covariance matrix to obtain $\{v_k, \lambda_k\}$ the eigenvectors and eigenvalues

respectively, which represent the principal directions in the tangent space $T_p\mathcal{M}$ and the variances.

Chapter 3

Greedy Principal Flows

3.1 Goal Of Research

The main objective for greedy principal flows is to quantify or describe multivariate data on the manifold: we cannot simply fit a line, as this is not Euclidean space. Instead, we want some curve or path such that, locally, it follows the path of maximal variation of the data in some neighbourhood, but globally also provides the path of maximal "cumulative" variation of the data. This problem has already been solved in [5], where the principal flows were constructed by solving a problem in variational calculus. Here we note that we focus on the 1st order principal flow, which can be thought of as the manifold extension of the 1st principal component in euclidean space. Therefore, we focus instead on constructing the principal flow using a novel, simpler to implement approach: a greedy algorithm. Thus, formally, our aim is to implement this simpler version of the principal flow algorithm in a popular programming language, and experiment with the results that this implementation of the principal flow algorithm. How would it describe various, popular multivariate datasets? Could it find novel ways of describing popular, existing high-dimensional data?

3.2 An explanation of the algorithm

Throughout we will assume that $\mathbf{X}$ lies on the hypersphere. To find our principal flow, we first need a starting point. Since our principal flow follows the path of maximal variation of our data, we know it should pass through the centroid of the data. Thus, we first aim to estimate this centroid. Although there are many ways of doing this, we opt to make use of the fact that the first principal component passes through the centroid of the data. Thus, if we iteratively project all the data onto the tangent space of the hypersphere, find the 1st principal direction, move in that direction, and find the projected point on the hypersphere, we will eventually converge on the centroid.

Centroid Algorithm:

1. Let $p = x_i$, a random data point.
2. Compute $log_p(x_i)$ for all x_i, and let these vectors be the rows of the matrix $\bar{\mathbf{X}}$.
3. Calculate the covariance matrix of $\bar{\mathbf{X}}$.
4. Diagonalise the matrix, then save the eigenvector corresponding to the largest eigenvector, $\mathbf{v}_1$.
5. Move in the direction of $\mathbf{v}_1$ a step size of ϵ, Let $p' = p + \epsilon \mathbf{v}_1$.
6. Then set $p = exp_p(p')$.

Then we start from that centroid, and build our principal flow from there. **Problem**: What if our data stretches all around the hypersphere? How do we deal with projecting data through the sphere?

Instead of taking all data into consideration, we choose a small neighborhood around our centroid, whose size is controlled by h. This neighbourhood is determined by some kernel function: either binary or gaussian. The binary kernel includes points in some neighbourhood and excludes points outside, while the gaussian kernel weights points according to the gaussian distribution based on their distance from the original point. Thus, we project the data within some neighbourhood $\mathbf{X}_h$ onto the tangent space at the centroid, p: $T_p\mathcal{M}$. We use the logarithm map, log_p to do this. Then the path of maximal variation in this neighbourhood of points is the first principal direction of this data from PCA. This direction is obtained by diagonalising the covariance matrix of the data on this tangent space.

Problem: This direction clearly is not accurate if we only move in this direction, since it will eventually lead us out of the surface of the hypersphere, and even on the hypersphere, the neighbourhood of points may differ, and change the direction of the path of maximal variation.

Thus, instead of only using this direction, we move infinitesimally in this first direction, then carry out the same procedure again. Thus we iteratively find the "local" direction of maximal variation, move in that direction, and re-compute the next direction of maximal variation. We continue doing this until we have obtained a flow through the entire data set. This does indeed follow the framework that isomap and LLE abide by as well: that obtaining the best option locally becomes the best option globally as well. This is exactly the idea of this Greedy Principal flow algorithm.

3.3 Algorithm Steps

We assume the underlying structure of the data is a hypersphere. Starting from the centroid of the data set (user defined or calculated below), we apply the following procedure:

1. Project the data residing on the hypersphere onto the hyperplane at p (initially the centroid of the data), $T_p\mathcal{M}$. We use log_p to do so, obtaining a matrix of vectors on the tangent plane that point from p to the projected points. These are the plane vectors.

2. Compute the covariance matrix of the plane vectors applying weights as necessary via the chosen kernel function: binary, gaussian, or identity. We note using the plane vectors is the same as finding the covariance matrix of the centered data. Since we

take each p as the current centroid of a neighbourhood of points we project onto the hyperplane, then each vector is $\mathbf{v} - p$.

3. Perform eigendiagonalisation of the covariance matrix. Take the eigenvector corresponding to the largest eigenvalue. This indicates the direction of the principle flow. Let us call it the principal direction.

4. If this is the first iteration, we simply use the principal direction as is. Otherwise, we check that this principal direction is in the same direction as the previous principal direction, and if not, apply a negative sign to the principal direction.

5. We take a small step in the principal direction on the plane, then use the exponential map to find the corresponding point on the sphere. Make this point the new p.

6. Repeat 1-5 for the point on the opposite end of the growing principal flow.

7. Store both points.

8. Repeat 1-7 until the maximum nunmber of iterations has been reached, or until there are no more points in the neighbourhood around p.

3.4 Extension: Greedy Principal Boundary

In the section above, we have already seen the principal flow. Now we extend the idea of Principal flows to attempt to find some boundary of the data. Let us assume that the data is contained on some ellipse of the manifold $\mathcal{M}$. Then our aim is to find some boundary around this ellipse. We proceed similarly to the principal flow, except that we also take the 1st and 2nd largest eigenvector and eigenvalues and use them to compute the boundaries of data.

Algorithm

1. Project the data residing on the hypersphere onto the hyperplane at p (initially the centroid of the data), $T_p\mathcal{M}$. We use log_p to do so, obtaining a matrix of vectors on the tangent plane that point from p to the projected points. These are the plane vectors.

2. Compute the covariance matrix of the plane vectors applying weights as necessary via the chosen kernel function: binary, gaussian, or identity. We note using the plane vectors is the same as finding the covariance matrix of the centered data. Since we take each p as the current centroid of a neighbourhood of points we project onto the hyperplane, then each vector is $\mathbf{v} - p$.

3. Perform eigendiagonalisation of the covariance matrix. Take the eigenvector corresponding to the largest eigenvalue. This indicates the direction of the principle flow. Let us call it the principal direction. We also save the 2nd eigenvector and its associated eigenvalue.

4. Use the eigenvalues obtained to calculate the radius of the ellipse of the data: where the radius is the 2nd largest eigenvalue divided by the largest eigenvalue. Then we move a distance of this radius multiplied by a user specified parameter in the direction indicated by the 2nd largest eigenvector and its opposite direction to obtain both boundaries. Store both boundary points.

5. If this is the first iteration, we simply use the principal direction as is. Otherwise, we check that this principal direction is in the same direction as the previous principal direction, and if not, apply a negative sign to the principal direction.

6. We take a small step in the principal direction on the plane, then use the exponential map to find the corresponding point on the sphere. Make this point the new p.

7. Repeat 1-6 for the point on the opposite end of the growing principal flow.

8. Store both principal flow points.

9. Repeat 1-8 until the maximum nunmber of iterations has been reached, or until there are no more points in the neighbourhood around p.

Chapter 4

Applications

Writing the algorithm is meaningless without testing that it also functions as we want it to. First we start with simple applications on toy data to confirm that our algorithm works as intended, then we apply it on some real world data to show how the principal flow can be used there as well.

4.1 Toy Data

4.1.1 Without Noise

As a sanity check or proof of concept of our principal flow, we first want to test our algorithm on some toy data that we know lies on the 3-dimensional unit sphere. This will help us visualise the flow created and determine if it follows the pattern of the data, and thus act as a proof of concept of our algorithm. We generate some data artificially.

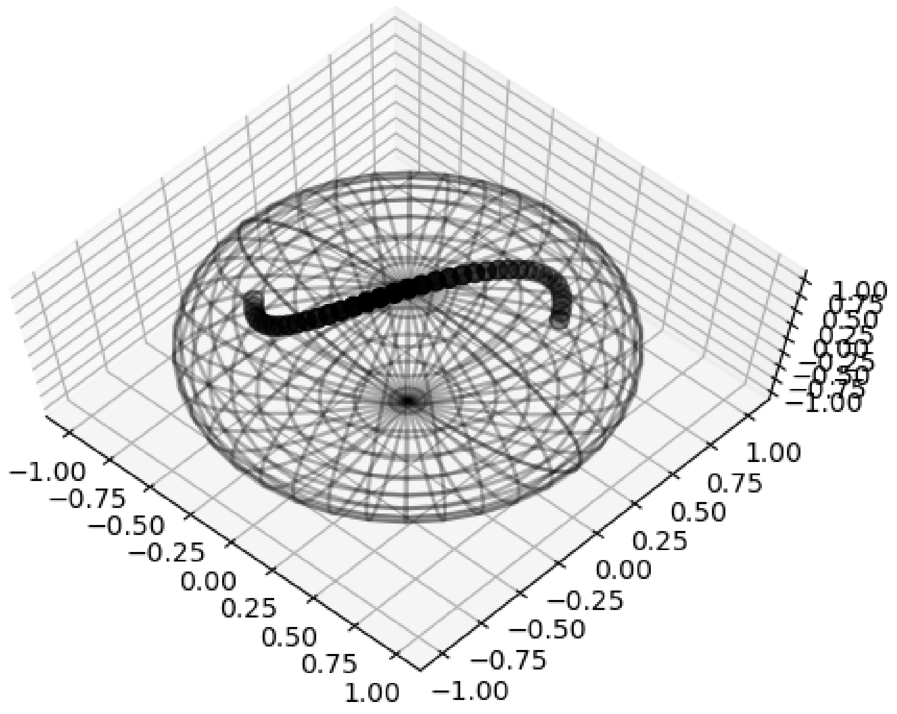

Figure 4.1: Toy data 13, $\mathbb{R}^3$

For example, this dataset is created by setting the first coordinate of the i-th point, $x_{i,1} = \frac{i-n/2}{n}$, then $x_{i,2} = sin(4 * x_{i,1})/2$, and the third to $x_{i,3} = \sqrt{1 - x_{i,1}^2 - x_{i,2}^2}$, where n is the number of points we want to generate.

Now that we have seen the Toy Data, let us apply the Principal Flow algorithm to the data above.

This 3D plot shows the original data in black, and the principal flow in red. With some tuning of h, the size of the neighbourhood, we can see that we have constructed a principal flow that follows the original data almost exactly, reconstructing an S with some slight differences at the curves of the s-shape of the original data. We have now seen that proof that our principal flow algorithm works: it is able to accurately reconstruct the toy data,

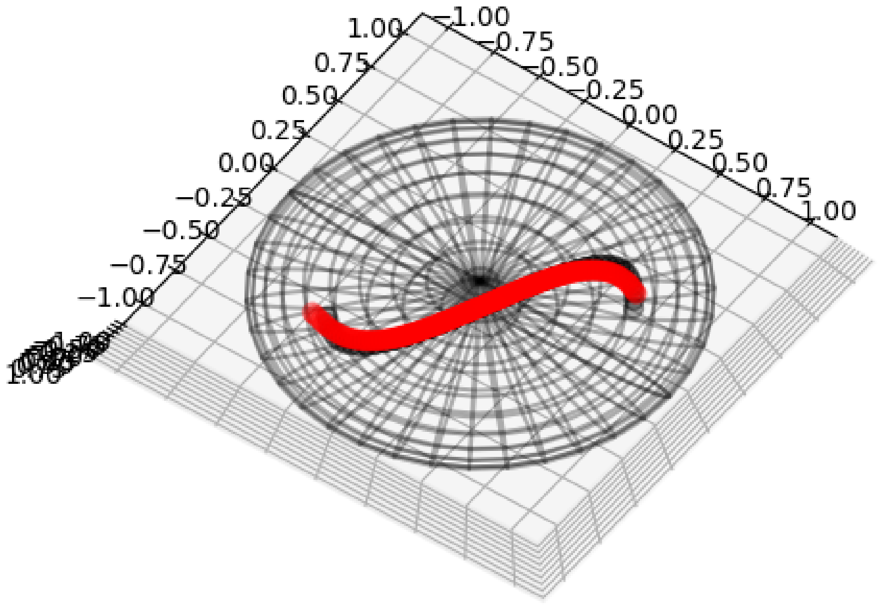

Figure 4.2: Principal Flow on Toy Data, $\mathbb{R}^3$

the s curve on the sphere.

4.1.2 With Noise

Next, gaussian noise was added to the S-shaped data on the sphere to create a noisy dataset. Then we fitted a principal flow to this noisy data. NOte: run noisy flow again! With same seed this time....

We can see that the principal flow obtained seems to follow the new pattern of variation in the data: from the more dense cloud of points on the left, to the curve of the points in the center to the other dense cloud of points on the right. We can see from these examples that even with noise, our algorithm is able to discern the pattern of the data.

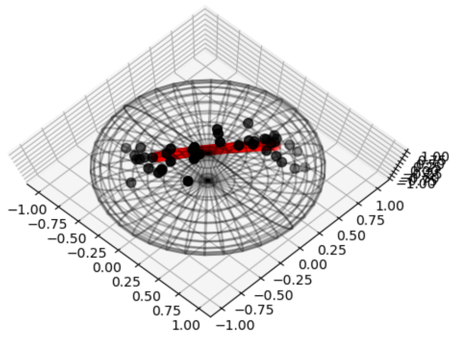

(a) Flow on Noisy Data using binary kernel

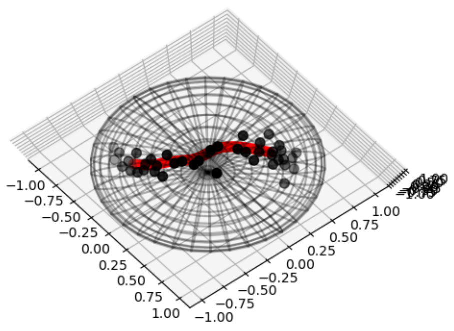

(b) Flow on Noisy Data using gaussian kernel

Figure 4.3: Illustration of a Tangent Space

4.1.3 Boundary Flow with Noise

Next we test out our extension, our algorithm for our principal boundary. Since we need a "cloud" of data, we apply some gaussian noise on the data from above, and then run our principal boundary algorithm on it. Let the principal flow be the curve in red, and the boundaries be in blue and green.

With some tuning, we obtain these 3 curves: we can see that the principal flow is in the middle of the dataset, while the boundary flows accompany it in parallel and even form to the shape of the cloud of data, bending outwards when there is a point beyond it. Through this graph, we can see how the principal boundary can work and be shaped by the shape of the cloud of data.

4.2 Real World Data

Our results on artificial data are promising, however, it means little if there are no real-world applications for our greedy principal flow.

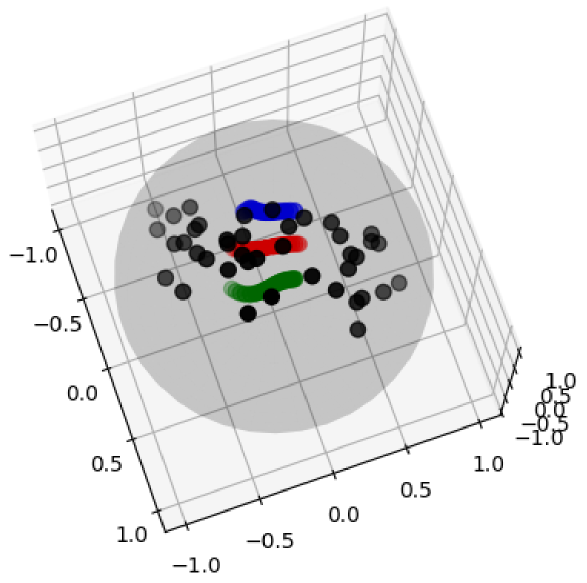

Figure 4.4: Boundary Flow on noisy data

4.2.1 MNIST

We first test the principal flow algorithm on the MNIST dataset, a rite of passage for machine learning algorithms. The MNIST dataset is a set of handwritten digits.

These images, read from left to right, top to bottom, are points from the principal flow. Although it does not represent all the variability of the 3s in the dataset, we can see that all the images obtained are "nice" representations of 3s, in that they cannot be confused with any other digit, and they seem to be relatively neatly written. Within these "nice" 3s then we observe the source of the variability: the "slant" of the digit. We can see that the digits start out leaning right and with a which starts out slanting to the right, and slowly rotates to slant to the left, going through a phase of being perfectly centered. This perhaps is an insight into the well-written 3s in the dataset and perhaps of neat handwritten digits in general: that they differ mainly in orientation. The fact that all the 3s on the principal flow are neat representations of the digit also suggests that our algorithm has found a path

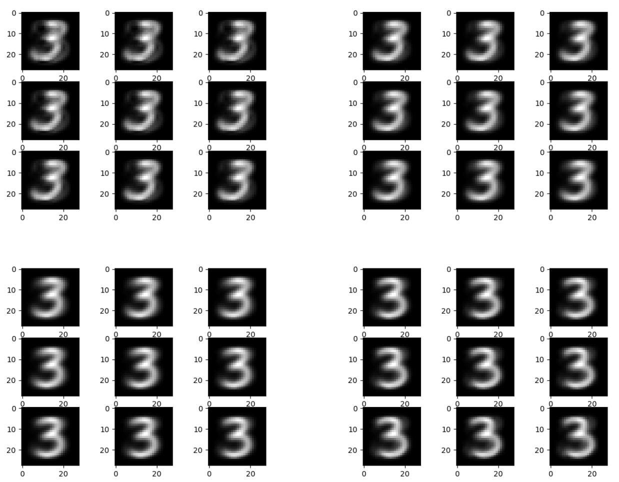
Figure 4.5: MNIST Flows, from left to right.

that has some intuitive meaning we can use to understand our data better, or perhaps that our choice of $\mathcal{M}^d$ was quite appropriate for this dataset.

4.2.2 Fashion MNIST

Next we test our principal flow on objects, and rather on 2 pieces of fashion that look quite alike: t-shirts and dresses.

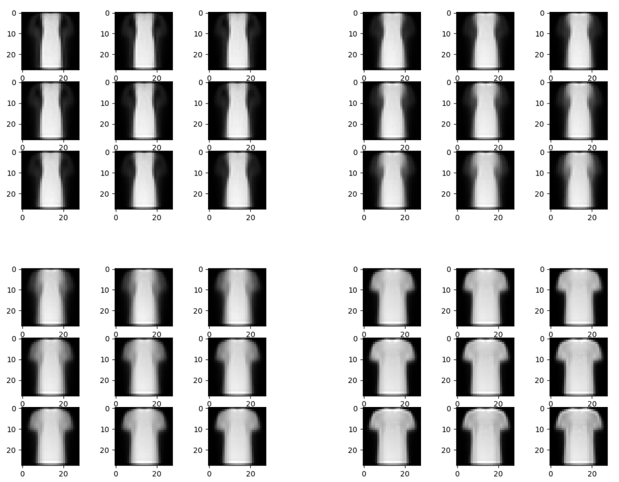
Figure 4.6: Fasion MNIST Flows, from left to right.

Here we can watch as dresses morph into t-shirts. More than just an interesting graphic, it shows that the principal flow is able to capture the variability of the data: here the data varies very clearly in the outline of the images, and images on the principal flow reflect this main source of variability. (do another transition between 2 objects)

4.2.3 Olivetti faces

Next we test our algorithm on a facial dataset. The Olivetti face dataset is old, and thus images are small, and only in black and white. This however is an advantage, as smaller images help the principal flow algorithm run faster, allowing us to experiment with a variety of parameters.

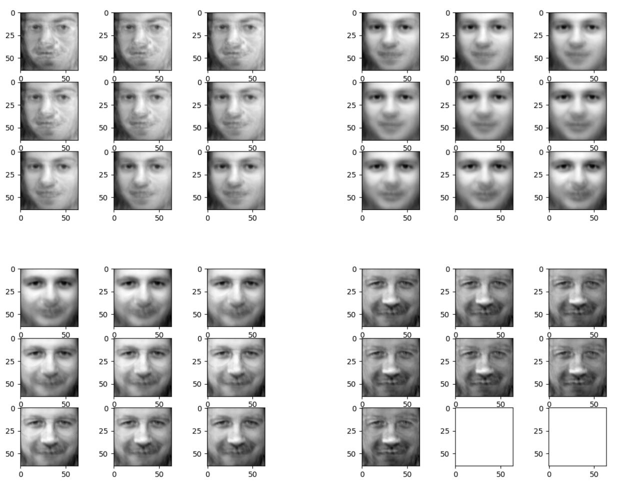

Figure 4.7: Flow for Olivetti face data, from left to right.

Although disturbing, we can see the results of our algorithm. The pictures we observe differ mainly on the angle of their face, and whether they have a beard. Indeed we observe that the difference between the men and woman in the data are not as stark as the difference between bearded and non-bearded individuals. This again indicates the strength of our algorithm: it is able to suss out the main way in which these images vary. Additionally, we can glean meaning from neighbouring images on the curve: they are close to each other in a meaningful way. We can see the series of faces transition from being slightly tilted away from the camera to facing the camera directly. The fact that the images on the principal flow transition smoothly tell us that a face slightly tilted away is near a face directly facing the camera which makes intuitive, real world sense. This is an indication that our choice of $\mathcal{M}^d$ does yield fruit and have some real world meaning, and that our principal flow seems to preserve some real world interpretation and meaning as it transitions smoothly through the orientation of faces in the data.

4.2.4 Faces in the Wild

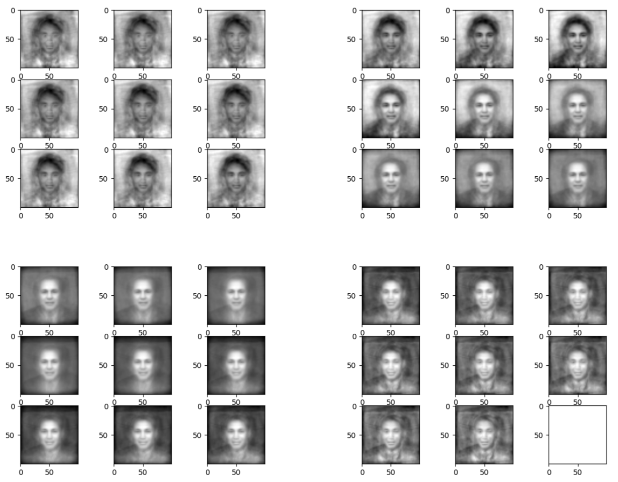

Figure 4.8: Faces in the wild flow, from left to right.

Here we test our principal flow algorithm on real faces with differing backgrounds, since these are photos found online. As with the cartoon faces, we can see that these faces differ in skin tone but also in eyebrow color, eye shape and background. This makes intuitive sense, since skin tone will determine a large portion of the face, and the background also takes up a large part of the images, and are likely to differ quite greatly.

Future Directions

The topic of principal flows and manifold learning in general is a rich field with much potential, and there are many avenues of expanding the work done in this report. One potential direction is constructing the k-th order principal flows, where $k > 1$. Another potential avenue of research is using different kinds of $\mathcal{M}^d$. In this report, we have restricted ourselves only to the hypersphere. Although this might be a "good enough" approximation, if we had intuition about the specific form of the manifold on which our multivariate data lies, and we determine that the hypersphere is unsuitable, then this current principal flow would not be able to accomodate this intuition. With a different manifold, we might be able to obtain a different principal flow that might give us more information about the variability of the data and describe it more appropriately than using the hypersphere. Additionally, we could also extend the greedy principal boundary to be a maximal margin classifier. Although this has already been done in [4], it has yet to be done with a greedy approach, and would be the first greedy maximal margin classifier for multivariate data lying on some Riemannian manifold.

4.3 Corrections

4.3.1 Abstract

Abstract too simple: can mention manifold data: higher dimensional mention multivariate data set: higher dimensional data but can be viewed as lying on a lower dimensional manifolds must explain principal flows in abstract. Must talk about hyperspheres more specifically explain why hyperspheres are there After rotation and centering and translation and normalisation, vectors can be viewed as points on the hyperspheres.

4.3.2 Motivation

seperately talk about programming language stuff in another paragraphed

4.3.3 Definitions

Remove the words denotes. $\mathbb{R}^D$ is the D-dimensional euclidean space.

Bibliography

[1] Ingwer Borg and Patrick J.F. Groenen (2005) ”Modern Multidimensional Scaling” , *Springer.*

[2] Fletcher, P. T., Lu, C., Pizer, S. M., and Joshi, S. (2004), ”Principal Geodesic Analysis for the Study of Nonlinear Statistics of Shape,” *IEEE Transactions on Medical Imaging*, 23, 995-1005.

[3] Tenenbaum, J. B., Vin de Silva, and Langford, J. C. (2000). ”A Global Geometric Framework for Nonlinear Dimensionality Reduction.” *Science*, 290: 2319-2323.

[4] Yao, Z., and Zhang, Z. (2019) ”Principal Boundary on Riemannian Manifolds.”

[5] Panaretos, V. M., Pham, T., and Yao, Z. (2014), ”Principal Flows,” *Journal of the American Statistical Association*, 109, 424-436.

[6] Saul, Lawrence K. and Sam T. Roweis (2003). “Think Globally, Fit Locally: Supervised Learning of Low Dimensional Manifolds.” *Journal of Machine Learning Research*, 4: 119–155. URL http://jmlr.csail.mit.edu/papers/ v4/saul03a.html.

[7]